Structures 15 (2018) 82–93

Contents lists available at ScienceDirect

Structures

journal homepage: www.elsevier.com/locate/structures

Evaluation of Self-Compacting Concrete Columns Reinforced with Steel and FRP Bars with Different Strengthening Techniques

Ahmed Hassan[a,*], Fouad Khairallah[b], Hala Mamdouh[b], Mahmoud Kamal[a]

[a] Department of Civil Engineering, Beni-Suef University, Egypt
[b] Department of Civil Engineering, Helwan University, Egypt

ARTICLE INFO

Keywords:
Column reinforcement type
Self-compacting concrete
Slenderness ratio
Strengthening and ductility

ABSTRACT

This study evaluates the overall behaviour of self-compacting short concrete columns with different reinforcement types. Major parameters, including reinforcement-type, confinement techniques and the slenderness ratio of columns, are studied. The FRP tube and spiral stirrups with two different volumetric ratios are considered as strengthening techniques. The mode of failure, axial compressive load, load-displacement curve, stress-reinforcement bars strain curve, ultimate, ductility and effect of the slenderness ratio are the main results obtained to evaluate the different column behaviours. The slenderness ratios have the same effect on column capacity for the different strengthening techniques, which have approximately 5% and 10% for the slenderness ratios of 6 and 8, respectively. The column capacity in the case of steel bars reinforcement is higher than when using FRP bars by approximately 22% of the column capacity. In terms of the reliability of different international code equations for the results of the tested columns, using CAN/CSA and ACI codes, discrepancies were noted between the steel and FRP as the main reinforcement for different code results. The columns reinforced by steel bars exhibit strong agreement with the ACI and Canadian specifications on the contrary FRP reinforcement, when neglecting its effect in these code recommendations.

1. Introduction

Columns are crucial components in most structures; hence, precise expectation of their capacity is vital for overall structural efficiency and reliability. Insufficient homogeneity of cast concrete as a result of segregation and poor compaction can certainly degrade concrete column performance. Self-compacting concrete (SCC) is used around the world due to its properties in the hardening and fresh states [1]. An extensive variety of uses for SCC have been reported in buildings, bridges, and tunnels since its first use in the early 1990s [2]. SCC is compacted under its own weight, without requiring vibration [3, 4], and it is suitable for concrete-filled tube columns, due to its rheological properties [5, 6]. Furthermore, SCC is suitable for use in difficult casting conditions or congested steel reinforcement sections [6]. Recently, various efforts have been made to evaluate the feasibility of using fibres in plain SCC [7–10]. After several years of discussion within the research community, fibre reinforced is now recognized as a structural material [11–13]. The combination of continuous re-bars and haphazardly disseminated chopped fibres in the matrix, generally referred to as hybrid reinforced concrete (HRC), has recently gained relatively high importance as a possible means of designing optimized structural elements [14, 15]. The use of steel fibre reinforcement, even in the incomplete substitution of conventional reinforcement, may allow for minimizing the construction time and costs that typically characterize the production process [16]. This study evaluates the use of steel and FRP reinforcement in self-compacting concrete columns. An experimental program is designed to investigate the possibility of using fibre bars as an alternative reinforcement for axially loaded columns. The overall behaviour of the columns is reported by recording the failure load, displacement and strains for the tested columns. Finally, this study examines the applicability of the different international codes of practice for design and construction on the experimental column results, using different reinforcement types.

2. Experimental program

2.1. Material properties

Trial Self–compacting concrete (SCC) mixes were prepared in order to achieve a 40 MP compressive strength. Development of the SCC involved using a high paste and low aggregate volume to endorse high deformability and reduce the risk of blockage and segregation during

* Corresponding author.
E-mail address: Ahmedhb96@eng.bsu.edu.eg (A. Hassan).

https://doi.org/10.1016/j.istruc.2018.06.003
Received 20 March 2018; Received in revised form 3 June 2018; Accepted 5 June 2018
Available online 15 June 2018

Table 1
Concrete mix proportions (unit: kg/m^3).

F_{cu} (MPa)	w/c ratio	Cement (kg/m^3)	Coarse aggregate (kg/m^3)	Fine aggregate (kg/m^3)	Silica fume (kg/m^3)	Sika ViscoCrete (kg/m^3)	Sika Fibre (G) (kg/m^3)
40	0.45	350	750	700	35	4	0.9

concrete placement manufacturing of the SCC columns. It basically differed from normal concrete mixes in terms of the coarse aggregate content and water-to-cement ratio, as well as the silica fume and additives used to manufacture the SCC. The concrete consisted of Portland cement, which is considered as Type I according to American Society for Testing and Materials ASTM, natural aggregates and natural water. Silica fume was used to increase the density, compressive strength and durability of the concrete, and also improve the fresh concrete performance with increased workability, and improved cohesiveness and stability. Sika ViscoCrete®-3425 is a third-generation super plasticiser for homogenous concrete, considered a powerful super plasticiser acting by means of different mechanisms. Sika Fibre is a monofilament polypropylene fibre for use in concrete mixes, which reduces the tendency for plastic and drying shrinkage cracking, improves abrasion resistance, reduces water migration, improves durability, reduces spalling, and increases the impact resistance of young concrete. Concrete mix proportions are listed in Table 1. Mixing was performed using a 0.125 m^3 concrete tilted rotating drum mixer. The dolomite, sand, silica fume and cement were dry mixed. Then, the water was gradually added with the Sika ViscoCrete-3425 and Sika Fibre, while mixing was performed for an additional 2 min, following which the concrete became homogeneous. Steel moulds were used to cast the concrete columns, and the concrete was cured by covering the columns with moist burlap sheets.

2.2. Description of test specimens

This study investigates the behaviour of SCC columns reinforced by steel and FRP bars with three different slenderness ratios. Eighteen circular columns specimens of 150 mm in diameter were tested and classified into three groups, as shown in Table 2. The main column reinforcement consists of 10-mm diameter steel and GFRP bars. The yield strength of the steel bars is 360 MPa, while the ultimate strength of the FRP bars is 800 MPa. For each column specimen, there exists a 6-mm bar diameter with cross sectional area A_{sp} equal to 28.27 mm^2 and volumetric ratio ρh (ratio of transverse confining steel volume to confined concrete core volume) equal to 0.034 for group G2, and 0.017 for group G1 and G3, to serve as the spiral stirrup. The third group is externally strengthened by FRP tubes. The different heights of the groups for studying the effect of slenderness ratio on the column behaviour are 120, 90 and 60 cm. The lateral reinforcement yield strength f_{yh} is 240 MPa. The column cross-sections and reinforcement details of the casted columns are displayed in Fig. 1. FRP tubes with a 150 mm inner diameter were provided by the Egyptian German Company (EGIC). These tubes were used in the confinement of the group G3 columns in this study. Properties of the FRP tubes are given in Table 3.

2.3. Test setup and instrumentation

A special 3D steel frame setup was constructed for testing the columns. The setup consisted of a load cell for reading the load value, head for fixing the specimen, and a linear variable differential transformer LVDT for measuring displacement. One steel strain gauge was used for the main steel bar at the mid-height of the column specimens, and all columns were tested under a concentric load. The test setup and instrumentation are illustrated in detail in Fig. 2.

Table 2
Column specimen properties and confinement techniques.

Group	Specimen designation	Ph (%)	Confinement technique	Height (cm)
G1	UCS4	1.7	Spiral steel hoops (control group)	60
	UCF4			
	UCS6			90
	UCF6			
	UCS8			120
	UCF8			
G2	HCS4	3.4	Spiral steel hoops	60
	HCF4			
	HCS6			90
	HCF6			
	HCS8			120
	HCF8			
G3	TCS4	1.7	FRP tube (FRP Tube)	60
	TCF4			
	TCS6			90
	TCF6			
	TCS8			120
	TCF8			

U Unconfined concrete.
T poly Tube.
H Steel hoops.
C Concentric load.
S Steel bars.
F Fibre glass bars.

3. Experimental results

3.1. Crack pattern and failure mode

The cracks and shape of failure are approximately similar in shape for the steel and FRP reinforcement columns within the same group for all groups; however, in the case of FRP reinforcement columns approaching failure, sounds were heard that indicated failure. A small vertical crack appeared in the lower and upper parts of the tested columns at approximately 0.63 of the failure load for groups G1 and G2. These cracks joined in the middle of the column at 0.90 of the failure load, with buckling in the main reinforced bars and spiral hoops leading to failure. For the columns strengthened with FRP tube, small black lines and a simple plastic tube bulge appeared in the lower and upper parts of the tested specimens following 0.68 of the ultimate load. As the load increased, these black lines increased in the longitudinal tube direction, up to 0.91 of the ultimate load. For heights of 60 and 90 cm, failure occurred in the columns' mid-height, while for the 120-cm height specimen, collapse occurred in the middle third of the specimen. The collapsed zones are approximately the same for the two groups, regardless of the high volumetric ratio. Based on the test results, the columns remain steady under concentric loads during the elastic load stage. When the elastic-plastic range is reached, the fibre tube begins to yield, and then lateral deformation emerges at the section of the column middle. The lateral deformation exhibits an obvious increase and the local bulge is found in the compressive area in the plastic range. Then, the concrete core is gradually crushed in the compressive area. For the failure load of the 60 cm columns, it is considered that the control specimen failure load is equal to 877.75 kN. Fig. 3 shows the cracks and failure mode of the tested columns. The slenderness ratios and strengthening techniques exert a noticeable effect on the column failure loads, and these effects are greater in the case of steel reinforcement than FRP reinforcement columns for different slenderness ratios, as shown in Fig. 4. Using FRP tubes in column strengthening for a limited high slenderness ratio failed, with global buckling occurring about the minor axis.

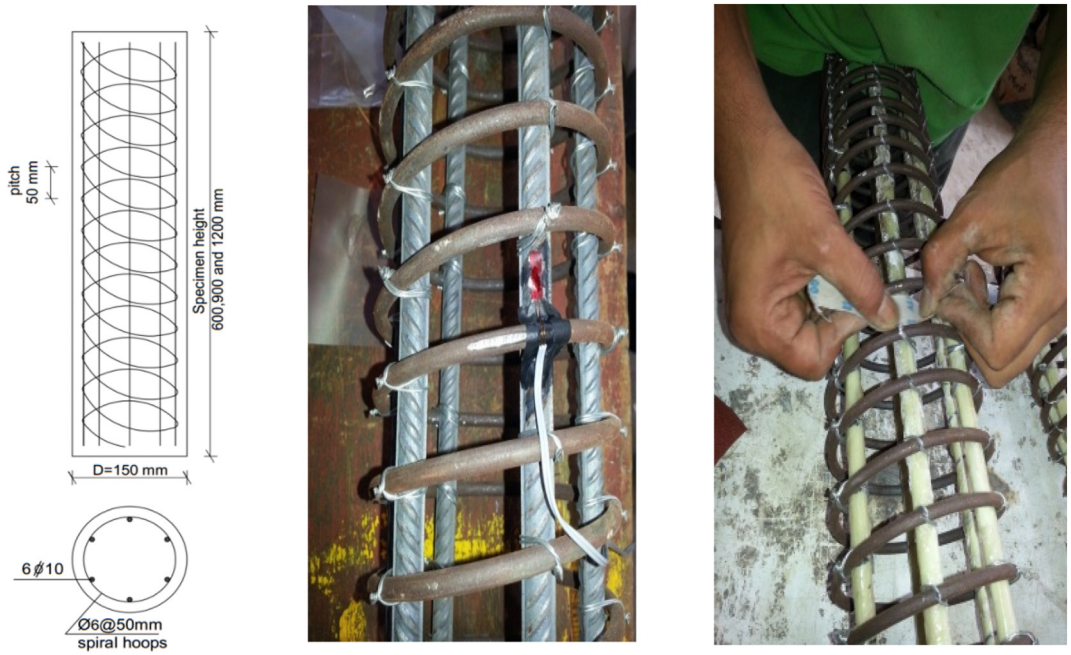

Fig. 1. Cross-section and reinforcement details of tested columns.

Table 3
Properties of FRP tubes.

Fibre type	Thickness t (mm)	Inner diameter (mm)	Outer diameter (mm)	Young's modules E (MPa)	Tensile strength f_u (MPa)
FRP tube	4.5	150	159	30,000	42

Fig. 2. Experimental test setup.

3.2. Effect of strengthening techniques on column behaviour

The experimental results of the ultimate strain for the longitudinal reinforcement, ultimate axial displacement, and ultimate load of groups G2 and G3, compared with the unconfined concrete columns of group G1 (the control group) are presented in Table 4. Generally, the FRP reinforcement columns sustained lower compressive strength values than those of the steel reinforcement column specimens by approximately 22% for different slenderness ratios and strengthening techniques, which may be attributed to the fact that steel reinforcement is often associated with a stronger bond with concrete compared to that of FRP reinforcement, which contributes only 10% of the column capacity [17]. The column capacity decreased with an increasing slenderness ratio in the tested column specimens. Furthermore, using different strengthening techniques demonstrated that the FRP tube increased the compressive strength in both the steel and FRP reinforcement columns by approximately 30%. Reducing the stirrups pitch in group G2 resulted in an increase in column capacity by 13.5% for steel and glass FRP reinforcement columns, from the control specimen capacity in G1. The tested columns with a slenderness ratio of 8 exhibited greater flexibility, which resulted in larger mid-height lateral displacement and lower stiffness.

3.3. Effect of slenderness ratio and strengthening type on column load-displacement

The load-displacement curve was approximately linear during the first stage, before the slope decreased, because of concrete stiffness reduction. The column stiffness was reduced due to the confined concrete cracking expansion. The columns sustained peak loads and axial displacements were shown in Figs. 5–7. The behaviours of the reinforced types affected the column capacity and failure mode by approximately 22%. A certain increase occurred in the displacement under a constant load, following which the displacement increased against the ultimate loads. Increasing volumetric ratio improved the short column behaviour to 40% during the elastic stage. The confinement of concrete by means of spiral hoop reinforcement increased the column capacity due to the spiral hoop reinforcement confining pressure. The outside concrete cover is not confined and will crush as the

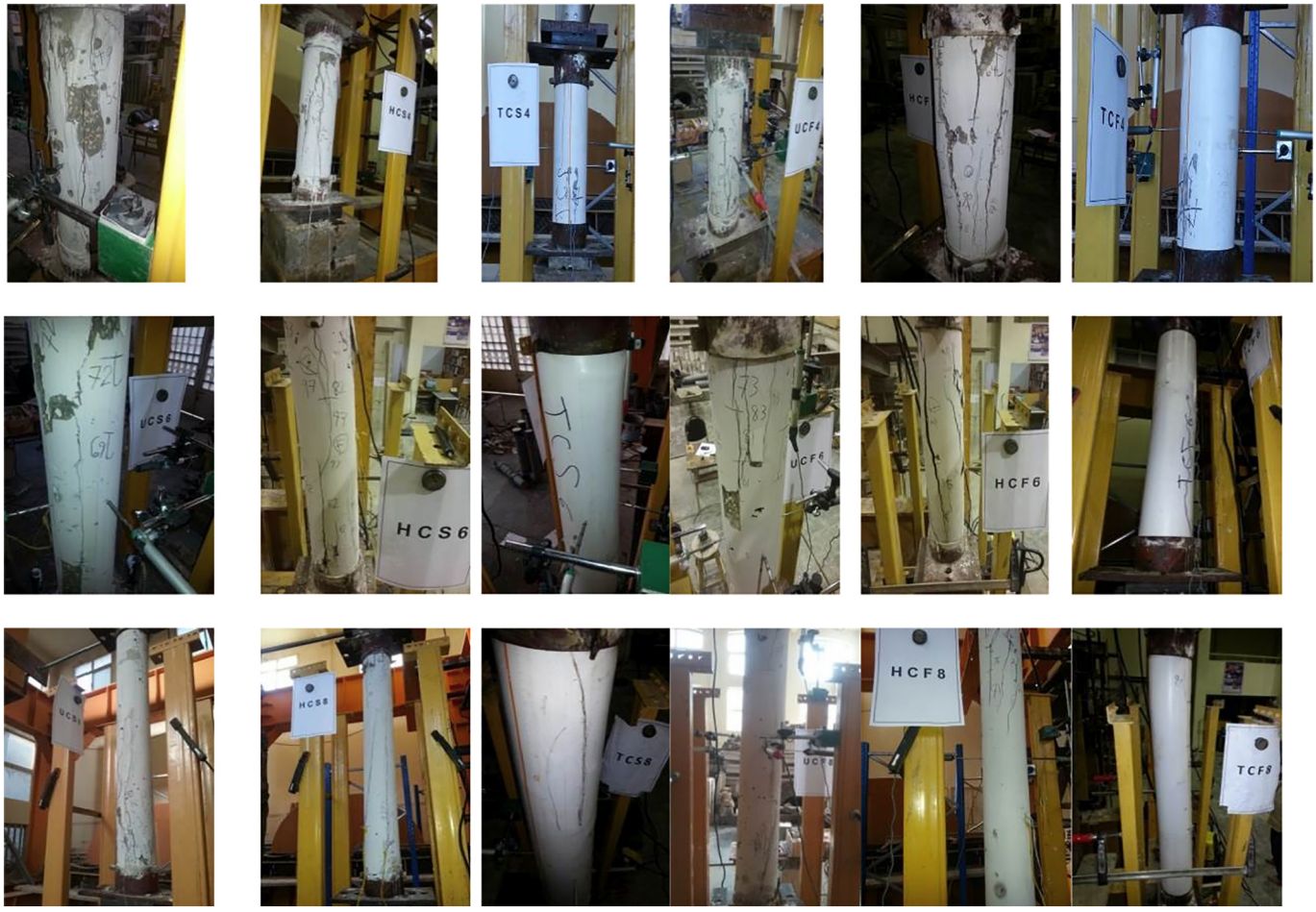

Fig. 3. Cracks and failure mode of tested columns.

concrete moves to its limiting strain, following which the spiral hoop reinforcement exerts an influence in confining the concrete and decreasing the extension of the concrete core. Strengthening by means of the FRP tube improves the overall columns behaviour, which increases the failure load by approximately 30% for all columns, while reducing the stirrups pitch improves the failure load to 13% for all columns. Delaying the occurrence of global buckling and reducing tube wall local buckling by means of FRP tube strengthening enhances the column capacity.

3.4. Effect of slenderness ratio and strengthening type on columns stress-reinforcement bar strain

The columns reinforced with steel and FRP bars exhibited similar axial strains; however, the columns constructed with steel bars demonstrated a higher ultimate strength than those reinforced with FRP bars, which may be attributed to the steel bars showing more ductile failure than the FRP bars reinforced under the same concrete strength and without a significant confinement technique. The first zone indicates a linear response rule for the unconfined concrete stiffness,

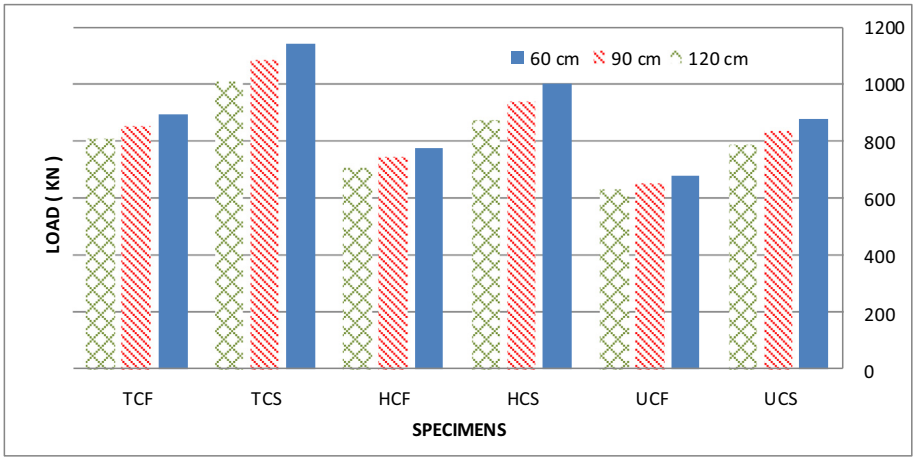

Fig. 4. Effect of slenderness ratio on ultimate load for tested columns.

Table 4
Experimental axial strain and compressive axial strength values for all tested columns.

Group no.	Specimen	Ultimate strain of steel bar	Maximum axial displacement (mm)	Ultimate load (kN)	Enhancement due to confinement (%)
G1	UCS4	0.0089	3.65	877.69	–
	UCF4	0.0088	3.2	678.62	–
	UCS6	0.01214	6.55	833.56	–
	UCF6	0.01204	5.95	651.16	–
	UCS8	0.01435	8.84	784.53	–
	UCF8	0.01395	7.88	627.62	–
G2	HCS4	0.01225	4.85	1000.27	13.97
	HCF4	0.0122	4.22	774.72	14.16
	HCS6	0.0148	7.85	936.53	12.35
	HCF6	0.01475	6.95	740.40	13.70
	HCS8	0.0169	9.65	872.79	11.25
	HCF8	0.01675	8.5	706.07	12.50
G3	TCS4	0.01502	5.55	1143.45	30.28
	TCF4	0.0149	4.95	892.40	31.50
	TCS6	0.01714	8.41	1078.73	29.41
	TCF6	0.01705	7.9	848.27	30.27
	TCS8	0.0194	10.45	1005.18	28.13
	TCF8	0.01925	9.35	804.14	28.13

which shows that no confinement is activated, while the axial strain in the longitudinal reinforcement is small. This stage reaches approximately 30 N/mm^2 for different strengthening techniques with a slenderness ratio of 8 for the steel and FRP bars columns, which exhibit close strains during the first stage. The increase in the column compressive strength and displacement length produced by the confinement on the FRP bar specimens is slightly higher than that of the steel bars specimens for all groups. Finally, the ultimate compressive strength and ultimate strain are accessed at the same point, and are variably improved depending on the confinement technique applied. Group G3 (confined with FRP tube) exhibits higher axial strain values for the steel bars and FRP bar columns than group G2 (double volumetric ratio), as shown in Figs. 8, 9 and 10.

4. Ductility

Ductility is dependent on different parameters related to rotation, curvature, deformation, deflection, and strain or absorbed and dissipated energy [18]. Generally, the ductility index μ,which depends on the energy absorbed, is used. The ductility of the steel and FRP reinforcement columns exhibited a significant difference in values depending on the column height and confinement technique applied. The ductility index μ is defined as Ap/Au, where Ap is the area under the load-displacement curve at peak load and Au is the area under the load-displacement curve before the load drops to 25% of the peak load [18]. The columns reinforced by steel exhibited larger ductility index values than the FRP reinforcement columns by approximately 20%. Slenderness ratios have a major effect on column ductility. Doubling the slenderness ratio from 4 to 8 reduced the ductility by 0.67 and 0.75 for the steel and FRP bar reinforcement, respectively, in group G1.

Decreasing the stirrups pitch has a maximum ductility improvement effect, more so than strengthening by tube, which results in the maximum improvement for ultimate load. The ductility improvement ranged from 54 to 84% and 37 to 51% for decreasing the stirrups pitch and tube strengthening, respectively, when using different slenderness ratios, as indicated in Fig. 11.

5. Reliability of different international code equations for tested column results

5.1. Equation codes for design column with steel bars reinforcement

The American code ACI 318-11 building code [19] introduces a formula for predicting the maximum loads for circular spiral columns. In an absolute axially loaded column, involuntary eccentricity occurs in the column section as the end condition and imprecision of the construction or experiment. In order to remove these factors, the ACI 318–11 building code applies a reduction factor of 15% in the maximum nominal load P_o for spiral columns, as shown in Eqs. (1) – (10). Fig. 12 illustrates the arch actions for a hooped circular column.

$$Pr = \varphi Po \qquad \text{for spiral columns } (\varphi = 0.75) \tag{1}$$

$$Po = 0.85\, fc'\,(Ag - Ast) + f\,y\,Ast \tag{2}$$

$$Po = 0.85\, fcc'\,(Ac - Ast) + f\,y\,Ast \tag{3}$$

$$fcc' = fc'\left(-1.25 + 2.25\sqrt{1 + \frac{7.9*\ f1'}{fc'}} - 2\frac{f1'}{fc'}\right) \tag{4}$$

$$f1' = f1^*\ k_e \tag{5}$$

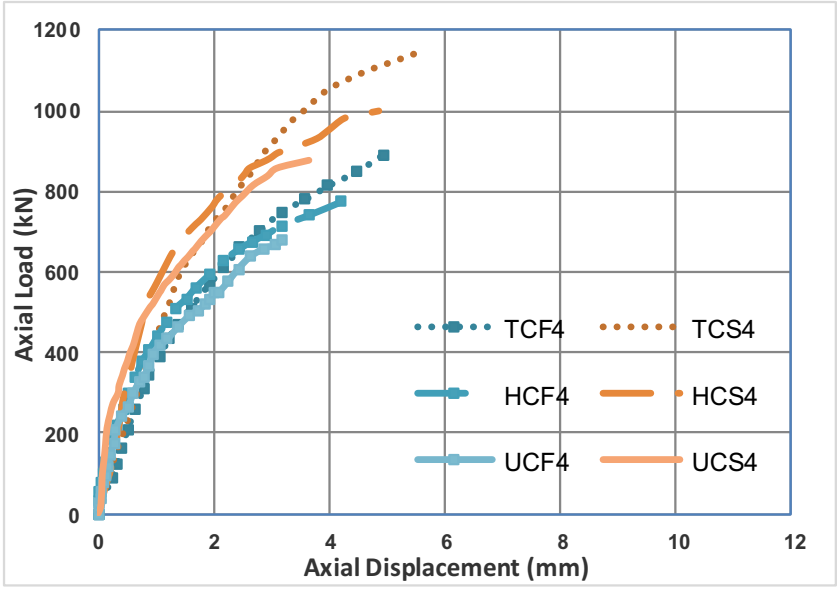

Fig. 5. Axial load-displacement according to confinement type (slender ratio 4).

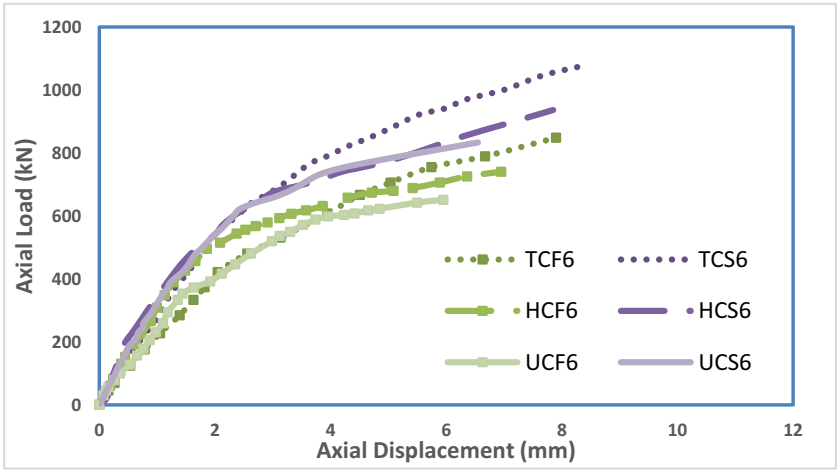

Fig. 6. Axial load-displacement according to confinement type (slender ratio 6).

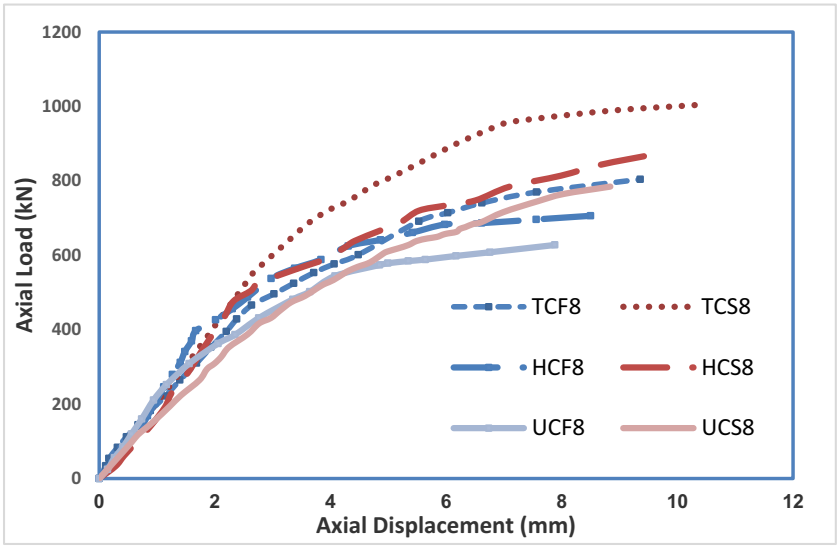

Fig. 7. Axial Load-Displacement according to confinement type (slender ratio 8).

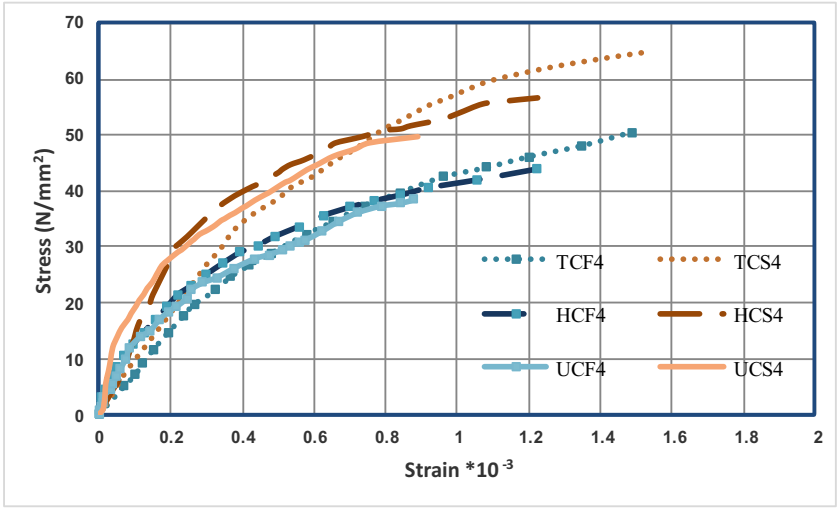

Fig. 8. Comparison of stress-strain curves according to confinement type (slender ratio 4).

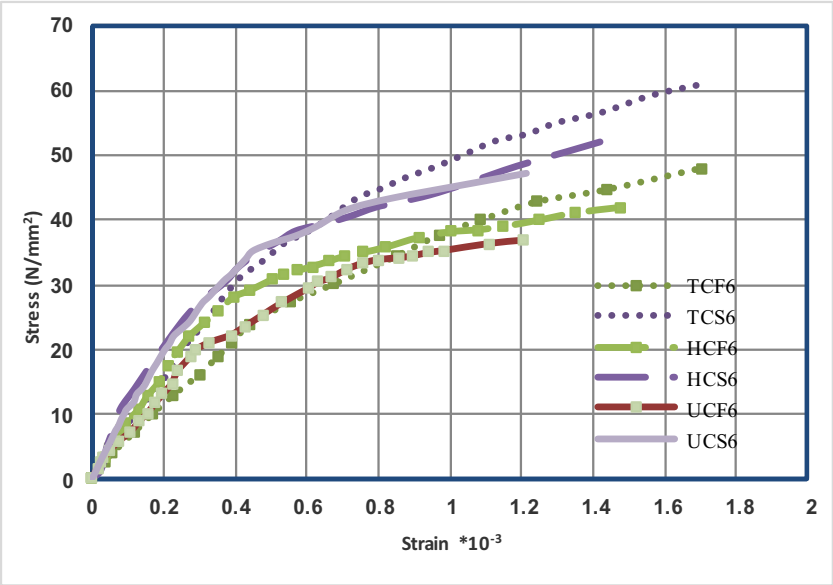

Fig. 9. Comparison of stress-strain curves according to confinement type (slender ratio 6).

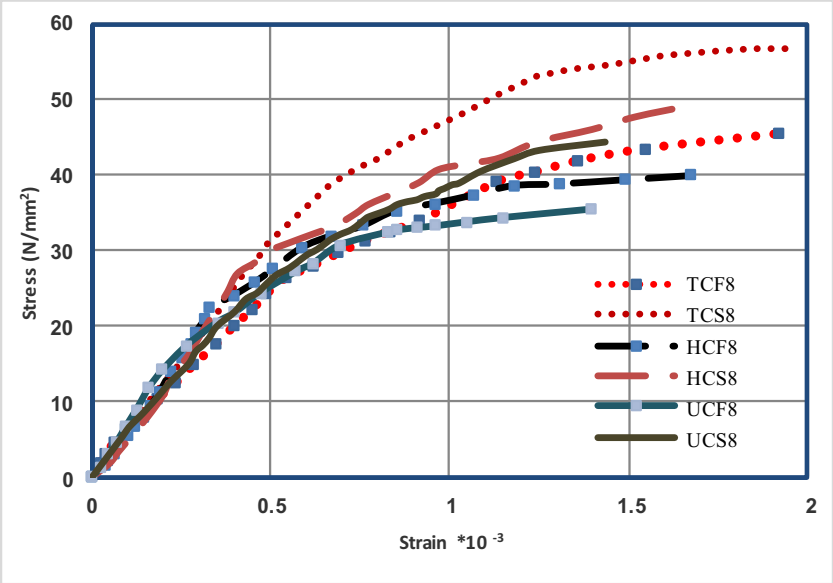

Fig. 10. Comparison of Stress-Strain curves according to confinement type (slender ratio 8).

$$\mathbf{ke = 1} \quad \text{columns confined with FRT tube} \tag{6}$$

$$f_l = \frac{2fut*t}{d} \tag{7}$$

$$f_l' = 0.5 f y_h ke\ \rho_S \quad \text{for circular spirals} \tag{8}$$

$$\mathbf{ke} = \frac{\left(\mathbf{1} - \frac{\mathbf{s'}}{\mathbf{2ds}}\right)}{(\mathbf{1} - \boldsymbol{\rho}\mathbf{CC})} \quad \textit{For spiral} \tag{9}$$

$$\boldsymbol{\rho}\mathbf{CC} = \frac{\mathbf{Ast}}{\mathbf{AC}} \tag{10}$$

Further equations are introduced by the CAN/CSA A23.3–04 Canadian code [20], which are approximately similar to the ACI 318–11 equations. The Canadian code proposes a resistance factor for steel and concrete materials instead of a reduction factor of the strength as specified in the ACI, as shown in Eqs. (11)–(14).

$$Po = \alpha 1\, fcc'(Ag - Ast) + f\ y\ Ast \tag{11}$$

$$Po = \alpha 1\, fcc'(Ac - Ast) + f\ y\ Ast \tag{12}$$

$$\alpha 1 = 0.85 - 0.0015 f\ c' \geq 0.67 \tag{13}$$

$$Pr = k\,[\alpha 1 \varphi c\ fc'(Ag - Ast) + \varphi s\ f\ y\ Ast] \tag{14}$$

where k strength reduction factor for unexpected eccentricities, which equal to 0.80, φc Resistance factor for concrete, which equal to 0.75, φs Resistance factor for non-pre- stressed reinforcing bars, which equal to 0.9.

The Euro code 2 [26] introduces charts according to columns slenderness as shown in Eqs. (15–22) for predicting the maximum design loads (P_r) for circular spiral columns. The suitable chart for the studied columns was shown in Fig. 13. The maximum nominal load P_o for spiral columns can get from P_r.

$$M_{Ed} = e_0{}^* N_{Ed} \tag{15}$$

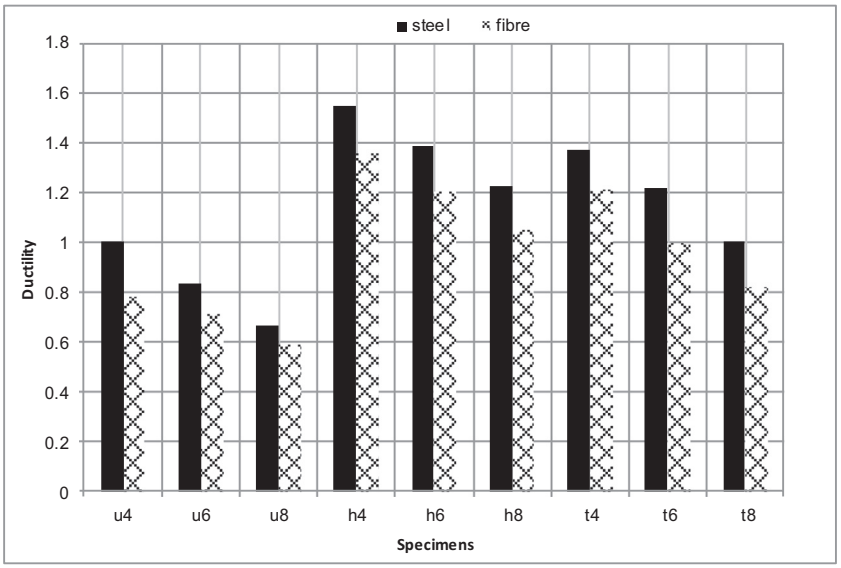

Fig. 11. Effect of strengthening type on column ductility.

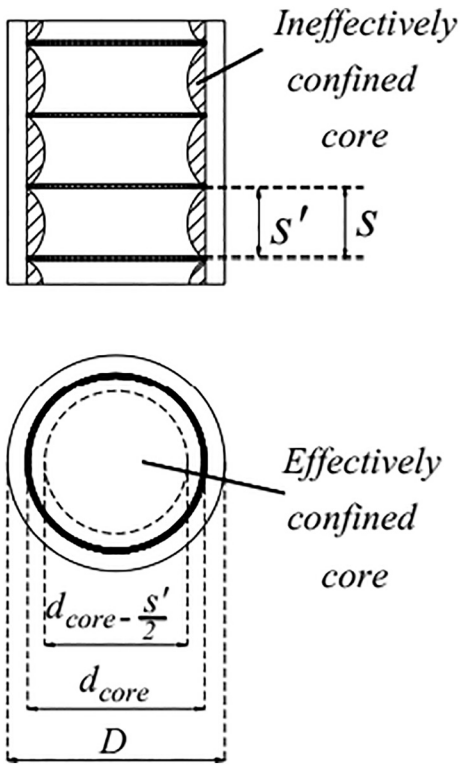

Fig. 12. Arch actions for hooped circular column.

$e_0 = h/30$ but ≥ 20 mm (16)

$\lambda = 4\, l_o/h$ For circular section (17)

$l_o = K\, l = 1^* 1200 = 1200$ mm for the highest column (18)

A = 0.7 (default) B = 1.1 (default) (19)

$C = 1.7 - -r_m = 1.7 - -M_{01}/M_{02} = 2.7$ for specimens (20)

$n = N_{Ed}/A_c\, f_{cd} = 1$ (21)

$\lambda_{lim} = 41.58$ (22)

$\lambda \leq \lambda_{lim}$ all column is not slender

Knowing As, Ac, Fcu and Fy and Using Fig. 13 to determine load which carrying by each columns.

The comparative studies using the tested columns results demonstrate that the results predicted for columns design loads by the Euro code are lower than those of the ACI equations and Canadian equations for columns strengthen by spiral steel hoops only, on contract of using poly tubes for externally strengthening produces the closest prediction of design loads in three different codes as reported in Fig. 14.

The slenderness ratios have a noticeable effect on the column results, and the ACI results are an overestimation of the experimental results. The calculated column ultimate strengths using the ACI 318-11 Euro code and CAN/CSA A23.3-04 codes are relatively conservative. The ACI 318-11 code produces the closest prediction, with an average of 20% higher, and is lower than the test results depending on the slenderness ratios applied. For tube strengthened columns, the tri-axial compression strength of concrete produces strong agreement with Euro code which close with the other codes by difference about 3% as reported in Fig. 15.

5.2. Equation codes for design column with glass FRP bars

FIB bulletin [11, 25] ignores the contribution of GFRP bars of such bars in carrying compression loads. CSA S806 [21] now permits the use of FRP bars as column longitudinal reinforcements under axial loads only, disregarding the effect of FRP bars in the ultimate capacity of columns, as shown in Eq. (24). Eq. (25) presents the ACI 440.6M-08 [22] design equation, ignoring the role of the FRP bars and using a reduction factor of 0.85. Certain studies have used two other methods, namely Eq. (26), to predict the nominal axial capacity of the FRP columns (Afifi, 2013) [23]. Eq. (26) was introduced to determine a value for the contribution of FRP bars using the reduction factor (α_g) [24]:

$Po = \alpha 1\, fcc'(Ac - AF)$ (Canadian [21]) (24)

$Po = 0.85\, fcc'(Ac - AF)$ (ACI [19]) (25)

$Po = 0.85\, fcc'(Ac - AF) + \alpha g\, f\, fu\, AF$ (Tobbi et al., 2012 [24]) (26)

A new factor (αg) was proposed to account for the decrease in compressive strength of the FRP bar as a function of its tensile strength. This factor was expected to be equal to 0.35, based on the data in [24].

Fig. 16 illustrates the relation of the experimental maximum load to the predicted nominal capacity (P_u exp/Pcalculated) of the specimens. These values indicate that this equation provides effective agreement

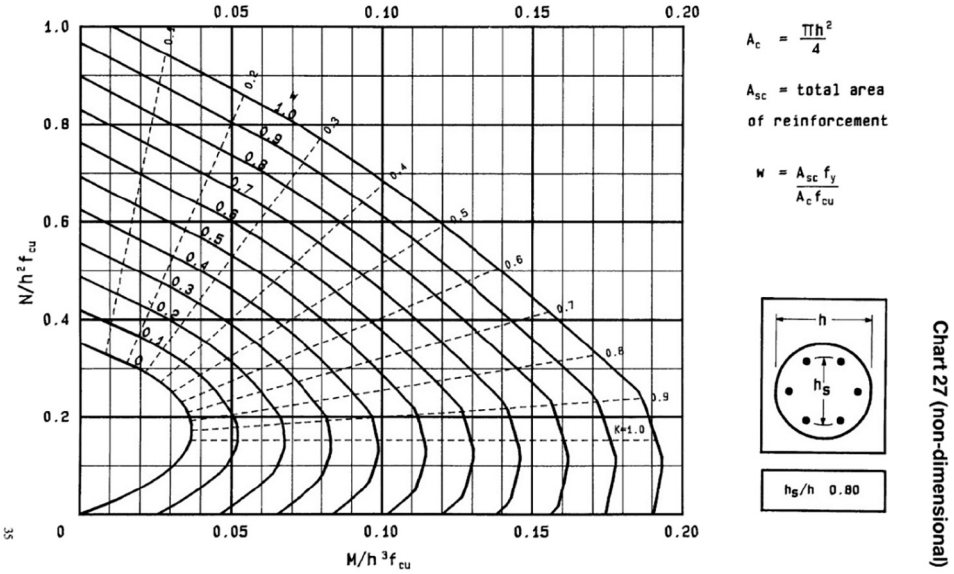

Fig. 13. Design curves for circular columns according to Euro codes [26].

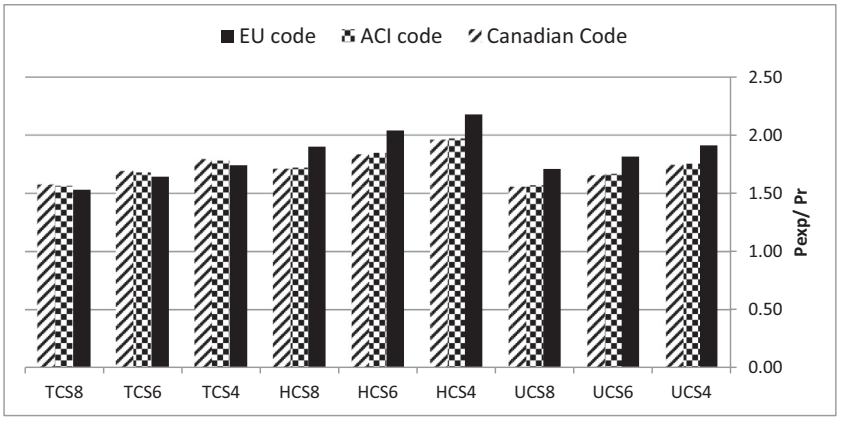

Fig. 14. Comparison of ACI code, Euro code and CAN/CSA code for column design load capacity.

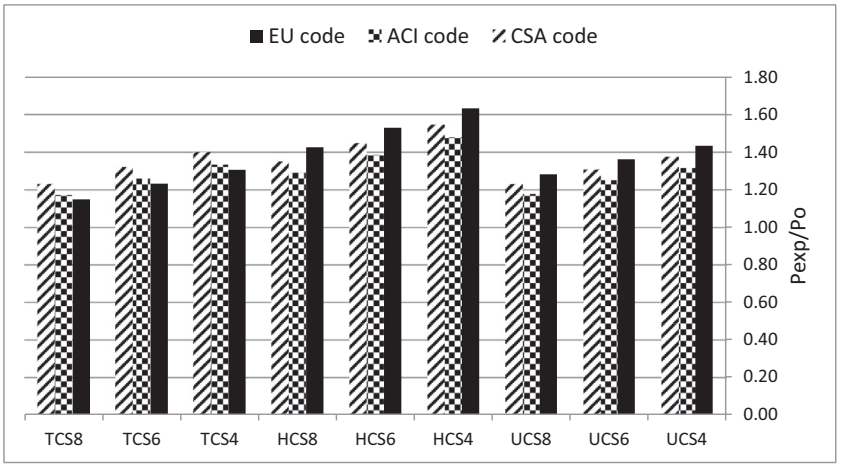

Fig. 15. Comparison of ACI code, Euro code and CAN/CSA code for column ultimate load capacity.

with the nominal capacity of the FRP reinforced columns. When ignoring the contribution of the FRP longitudinal bars in the Canadian equation, the values range from 160 to 1.24 while Euro code range from 1.82 to 1.20 and with the ACI equation they range from 1.37 to 1.17, as indicated in Fig. 16. The ratios of the experimental maximum load to the predicted values using Eq. (26) range from 1.18 to 0.98. Increasing volumetric ratio of spiral steel hoops and using poly tube to strengthening the columns increase the reliability of Eq. (26) [24]. The expected factor should be equal to 0.35, and based on the data in [24], it is critical for a column slenderness ratio of 8 and spiral steel hoops with

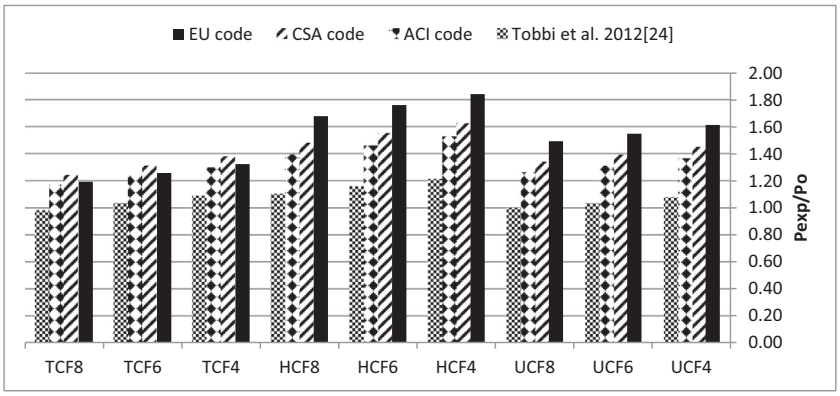

Fig. 16. Comparison of Canadian, ACI, Euro codes and Eq. (14) (Tobbi et al. 2012 [24]) for column load capacity.

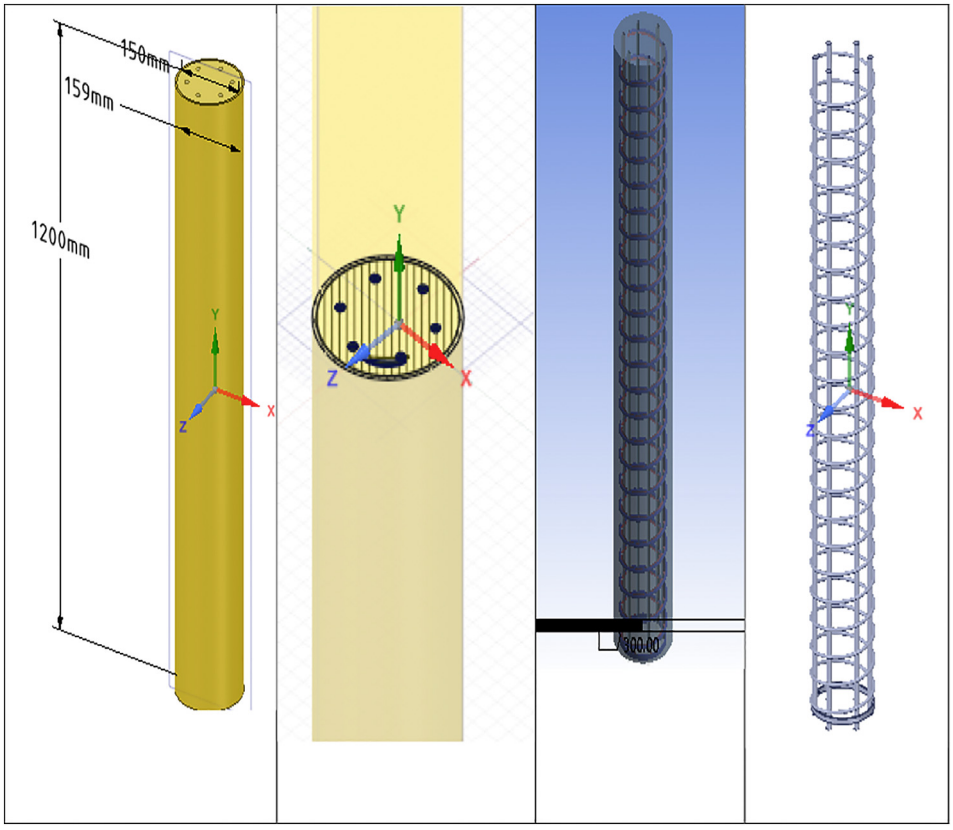

Fig. 17. Geometry of tested models.

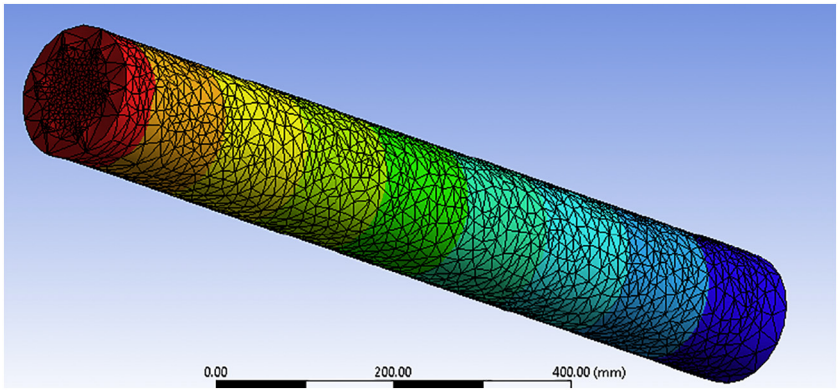

Fig. 18. Axial displacement for UCF8.

Table 5
Analytical and experimental results for 1200 mm columns.

Specimen	Experimental		Theoretical			Puexp/putheo
	Maximum axial displacement (mm)	Ultimate Load (KN)	Maximum axial displacement (mm)	Ultimate load (KN)	Confining stresses Mpa	
UCS8	8.84	784.53	8.22	756	45.5	1
UCF8	7.88	627.62	7.31	598	43.2	0.95
HCS8	9.65	872.79	9.24	860	58.2	1.28
HCF8	8.5	706.07	8.18	687	56.5	1.30
TCS8	10.45	1005.18	9.98	1001	68.7	1.51
TCF8	9.35	804.14	9.04	798	66.6	1.54

volumetric ratio 1.7; therefore, this factor should be decreased to 0.28 to cover all slenderness ratios with different strengthening techniques.

6. Finite element modeling of the specimens

The finite element method has emerged as the most powerful general numerical program Ansys. The reinforced concrete columns of height 1200 mm, width 150 mm diameters was modeled as a three dimensional system as shown in Fig. 17. The element is capable of plastic deformation, cracking in three orthogonal directions and crushing. GFRP or Steel bars were modeled by element embedded in the adjacent concrete mother element. Material properties can be input from the experimental investigations for 1200 mm columns height by different strengthening techniques of elements or each individual element, if needed. For different phenomena to be simulated, different sets of material properties are required. For example, the Young's modulus and strength are required for the stress analysis of solids and structures, Experiments are generally required to accurately determine the property of the materials to be used in the system. All numerical models are analyzed under centric loaded. Axial displacement was the recorded deformation to circular columns reinforced by GFRP bars as shown in Fig. 18. Table 5 compares the ultimate loads and axial deformations from the test columns and the finite element analysis. The results in Table 5 Indicate that the final load predictions obtained from the finite element simulations were close to the ultimate loads of the experimental results. Confining stress increased to 128% by increasing the volumetric ratio from 1.7 to 3.4 while using poly tube as columns confining increased the confining stresses to 151%.

7. Conclusions

1- Using FRP reinforcement instead of steel reinforcement reduced the column capacity by approximately 22% for different slenderness ratios of short columns and different strengthening techniques.
2- Slenderness ratios have a noticeable effect on steel and FRP reinforcement types in terms of column capacity.
3- Strengthening by tube achieved the highest compressive strength enhancement of approximately 30% for steel and glass FRP reinforcement columns, while increasing the volumetric ratio of spiral steel hoops increased the column capacity by 13.5% for the steel and FRP reinforcement columns.
4- Increasing the volumetric ratio of spiral steel hoops in the columns introduced the highest ductility with 46%, while poly tube strengthening columns exhibited improved ductility by 37% compared to unconfined columns.
5- Steel reinforcement columns introduced an approximately 20% greater ductility than FRP reinforcement columns in all tested groups.
6- The columns confined with spiral stirrups may have a small effect on column capacity; however, the benefit is increased ductility.
7- The results of the steel reinforcement in columns exhibit strong agreement with the Euro code, ACI and Canadian specifications, as opposed to FRP reinforcement.
8- The calculated column strengths using the Euro codes, ACI 318-11 and CAN/CSA A23.3-04 codes are relatively conservative for short columns.
9- The effective results obtained by increasing the volumetric ratio of spiral steel hoops should be considered in different code design equations.
10- The expected factor for FRP reinforced bars should be equal to 0.35 based on the data in [24], and is critical for a column slenderness ratio of 8; therefore, this factor should be decreased to 0.28.
11- Using the ANSYS software for the analysis of Steel and GFRP reinforced Columns under centric load is possible and can produce acceptable predictions throughout the load range in terms of ultimate load and axial displacement.

Nomenclature

P_h	Percentage of steel hoops in specimen
4-6-8	h/d slenderness ratio
$f_{cc'}$	Maximum concrete strength, concrete-to-concrete cylinder strength
$f_{c'}$	Specified compressive strength of concrete
A_g	Gross area of concrete section
A_{st}	Area of longitudinal reinforcement
f_y	Specified yield strength of transverse reinforcement
s′	Clear vertical spacing between hoops
d_s	Diameter of core measured centre-to-centre of hoops
ρ_{cc}	Ratio of area of longitudinal reinforcement to area of core of section
$f_{1'}$	Effective lateral confining pressure
k_e	Confinement effectiveness coefficient
f_1	Lateral pressure from transverse reinforcement, assumed to be uniformly distributed over surface of concrete core
ρ_s	Ratio of volume of transverse confining steel to volume of confined concrete core
F_{yh}	Yield strength of transverse reinforcement
A_{st}	Area of longitudinal reinforcement
A_c	Area of core concrete section
F_{ut}	Ultimate tube strength
t	Thickness of tube
d	Diameter of column

References

[1] EFNARC. Specification and guidelines for self-compacting concrete. Surrey, UK: European Federation of Suppliers of Specialist Construction Chemicals (EFNARC); 2002http://www.efnarc.org.
[2] Okamura H, Ouchi M. Self-compacting concrete. J Adv Concrete Technol 2003;1(1):5–15.
[3] Goodier CI. Development of self-compacting concrete. Proc Inst Civil Eng Struct Build 2003;156(4):405–14.
[4] Krishna N, Narasimha A, Ramana I, Vijaya M. Mix design procedure for self compacting concrete. Thin-Walled Struct January 2017;110:27–34.
[5] M. Mahgub, A. Ashour, D. Lam, X. Dai. Tests of self-compacting concrete filled elliptical steel tube columns. Thin-Walled Struct., 42(9), 1357–1377. doi:https://doi.

org/10.1016/j.tws.2016.10.015.
[6] Roeder CW, Lehman DE, Bishop E. Strength and stiffness of circular concrete-filled tubes. J Struct Eng 2010;136(12):1545–53.
[7] Mastali M, Dalvand A, Sattarifard AR. The impact resistance and mechanical properties of reinforced self-compacting concrete with recycled glass fibre reinforced polymers. J Clean Prod 2016;124:312e24.
[8] Mastali M, Dalvand A. Use of silica fume and recycled steel fibres in self-compacting concrete. Constr. Build. Mater. 30 October 2016;125:196–209. http://dx.doi.org/10.1016/j.conbuildmat.2016.08.046.
[9] Ghernouti Y, Rabehi B, Bouziani T, Ghezraoui H, Makhloufi A. Fresh and hardened properties of self-compacting concrete containing plastic bag waste fibers (WFSCC). Constr Build Mater 1 May 2015;82:89–100. http://dx.doi.org/10.1016/j.conbuildmat.2015.02.059.
[10] Yang S, Yue X, Liu X, Tong Y. Properties of self-compacting lightweight concrete containing recycled plastic particles. Construction and Building Materials 1 June 2015;84:444–53. http://dx.doi.org/10.1016/j.conbuildmat.2015.03.038.
[11] Fib Bulletin 65. Model Code 2010 – Final Draft. 1. 2010. p. 350. (ISBN: 978-2-88394-105-2).
[12] German Committee for Structural Concrete DAfStb Committee for Structural concrete. DAfStb guideline steel fiber reinforced concrete; 2012.
[13] Prisco M, Plizzari G, Vandewalle L. Fiber reinforced concrete: new design perspectives. Mater. Struct. November 2009;42(9):1261–81. http://dx.doi.org/10.1617/s11527-009-9529-4.
[14] Chiaia B, Fantilli A, Vallini P. Combining fiber-reinforced concrete with traditional reinforcement in tunnel linings. Eng Struct July 2009;31(7):1600–6. http://dx.doi.org/10.1016/j.engstruct.2009.02.037.
[15] Barros JAO, Taheri M, Salehian H. A model to simulate the moment–rotation and crack width of FRC members reinforced with longitudinal bars. Eng. Struct. 1 October 2015;100:43–56. http://dx.doi.org/10.1016/j.engstruct.2015.05.036.
[16] A.M. Shende, A.M. Pande, M. Gulfam Pathan. Experimental study on steel fiber reinforced concrete for M-40 Grade. Int Refereed J Eng Sci (IRJES) ISSN (Online) 2319-183X, (Print) 2319-1821 1(1) (2012), PP. 043–048.
[17] Afifi M, Mohamed H, Benmokrane B. Axial capacity of circular concrete columns reinforced with GFRP bars and spirals. J Compos Constr February 2014;18(1). http://dx.doi.org/10.1061/(ASCE)CC.1943-5614.0000438.
[18] Park R. Ductility of structural concrete. V62. Stuttgart: International Association for Bridge and Structural Engineering, IABSE Reports; 1991. p. 445–56.
[19] American Concrete Institute (ACI) Committee 318. Building code requirements for structural concrete and commentary ACI 318R-11 2011. [Farmington Hills, Michigan].
[20] Canadian Standards Association (CSA). Technical committee on reinforced concrete design A23.3-04, Rexdale, Toronto 2004.
[21] Canadian Standards Association (CSA). Design and construction of building components with fiber reinforced polymers CAN/CSAS806-12 2012. [Rexdale, Toronto].
[22] American Concrete Institute (ACI) Committee 440. Guide for the design and construction of concrete reinforced with FRP Bars ACI 440.1R-06 2006. Farmington Hills, Michigan].
[23] Afifi Mohammad. Behavior of circular concrete columns reinforced with FRP bars and stirrups Doctor of Philosophy Diss Université de Sherbrooke; 2013.
[24] Tobbi H, Farghaly AS, Benmokrane B. Strength model for concrete columns reinforced with FRP bars and ties. ACI Struct J 2014;111(4):789–98.
[25] Fib. FRP reinforcement in RC structures, technical report prepared by a working party of task group 9, FRP(Fiber Reinforcement Polymer) reinforcement by concrete structures. 2007.
[26] Eurocode 2. Design of concrete structures, part 1–2: general rules–Structural Fire Design, prEN 1992-1-2. 2002.